Nested Wire Array Z-Pinch Experiments Operating with 800 ns Implosion Time for Production of Aluminum K-Shell Radiation. First Results on the 1 MJ SPHINX Generator[1]

F. Lassalle[a], F. Bayol, C. Mangeant, F. Hamann, P. L'Eplattenier, G. Avrillaud*, H. Calamy, J.P. Bedoch, J.F. Cambonie, Y. Cazal, P. Combes, A. Morell, S. Ritter

Centre d'Etudes de Gramat, 46500 Gramat, France
** ITHPP, 46500 Thegra, France*
[a] *Phone: 33-5-65-10-54-13, Fax: 33-5-65-10-54-13, lassallf@cegramat.fr*

Abstract – Preliminary experiments have been done at Centre d'Etudes de Gramat (CEG) to analyze the performances of plasma radiation sources with implosion time up to 800 ns. SPHINX generator has been used to implode single and nested aluminum wire-arrays Z-pinches in µs direct drive mode with maximum current 3.4MA to 3.8 MA. The benefit of using nested arrays configuration was proved for the stabilization and reproducibility of the source. The dynamic of the implosion is studied with 1D & 2D visible cameras and X-UV time-integrated pin-hole cameras. The X-ray emission is qualified with time resolved resistive bolometry, filtered detectors (diamond PCDs, XRDs) and time integrated crystal spectrometer. Models for the 0D simulations are presented. Results show more than 10kJ of energy radiated above 1 keV, with pulse widths of 30–50 ns for a total radiation yield around 100kJ.

1. Introduction

The study of plasma radiation sources (PRS) has been a rich field during the last several years with the advent of reliable high current pulsed power generators. The main applications concern radiation effects, inertial confinement fusion and astrophysics that all need a high output power and fast X-ray pulses. Development of long implosion time Z-pinches is of great interest, at least for radiation effects studies that do not need too short X-ray pulses, because of their potential to reduce the complexity and cost of generators. Recent advances made by several laboratories in Z-pinch wire array designs and operations show that good K-shell yield can be achieved with up to ~300 ns implosion time [1–3], three times longer than the ~100 ns implosion time of typical Z-pinches obtained classically on capacitive storage generator as Saturn and Z at Sandia National Labs. CEG is investigating the performances of such sources with an other step increase in implosion time: up to 1 µs [4]. SPHINX generator (stored energy 1MJ, current rise time 1 µs), described in detail elsewhere in this conference [5], is used to implode single and nested aluminum wire arrays Z-pinches in direct drive mode with maximum current 3.4 MA to 3.8 MA (max current is 5.2 MA in 1.2 µs on a 5.5 nH short-circuit load). It actually uses 12 LTD branches charged at 50 kV, and it will be upgraded to 16 branches with charging voltage increased up to 70–75 kV in the next 2 years.

2. Experimental Configuration and Diagnostics

This first experimental series were carried out by varying, in a quite large characteristic range, the design of the source. We used single or double nested arrays with the following characteristics: height 3 or 5 cm, outer radius 6 or 7.5 cm, inner radius 3 or 3.7 cm, outer mass 0.18 to 2.2 mg, inner mass 0.5 to 1.1 mg, outer wires number 16 to 216 , inner wires number 40 to 92 (10.4 µm diam. Al wires) The configurations were chosen to have an implosion time between typically 600 to 800 ns. Sixteen ports are available for diagnostics in-between 2 LTD branches (but 2 occulted by the inductive supports of the convolute). The dynamic of the implosion is studied with a 1D optical streak camera with radial resolution and a 2D optical framing camera (Imacon: 8 images at 10 ns exposure, 2 images were out of service during these experiments). The X-ray output of wire arrays pinches is qualified using several diagnostics. Radiated Aluminum yields above ~1 keV (including Kshell and continuum) are measured using filtered photoconducting diamonds detectors (PCDs) and a filtered gold bolometer[2]. The total radiated yield is obtained with a bare Nickel bolometer [6]. Time-resolved power estimates in X-UV and for x-rays above 1 keV are obtained from the PCDs and a vitreous carbon cathode x-ray diode (XRD). Solid angles of observation of the detectors are corrected according to the experiment geometry and the hypothesis of a lambertian cylindrical emitter to determine the total outputs from the source [7]. Lines of sight have a 5° angle with the perpendicular of the pinch to reduce debris and plasma

[1] This work was supported by French Ministry of Defense/SpNum-ATM under contract N°0279507.
[2] Loan from the Sandia National Labs through the DOE/DGA "Lab to Lab" agreement.

pollution on the detectors. Spatial properties of the Z-pinch are studied with filtered time-integrated multi pin-holes camera. First results on spectral information has just been obtained with a time integrated crystal spectrometer (KAP) with axial resolution. All the x-rays detectors are protected with fast closing valves (1.5 ms closing time, located 4 to 5 m from pinch) [8].

3. Experimental Results

Single (5 to 7.5 cm radius) wire array loads were first tested [9]. They were producing large burst of UV (more than 200 ns FWHM) and a large X-ray pulse above 1keV (up to 100 ns wide) but the K-shell outputs stayed under 5 kJ for implosion times between 640 to 890 ns. They proved to be very unstable on the time integrated pin-hole images, not reproducible and stayed very far from 0D predictions using MQK or TWG radiation models. So we quickly moved to double nested arrays (named 'DS') in order to improve the dynamics and the stability of the implosion.

Implosion dynamics: 2D visible images (done through apertures in the return current post) are very instructive at a first level to understand the global phenomenology of the implosion. Fig. 1 presents an example of one of the first DS shots where these images are correlated to the current and X-rays powers histories.

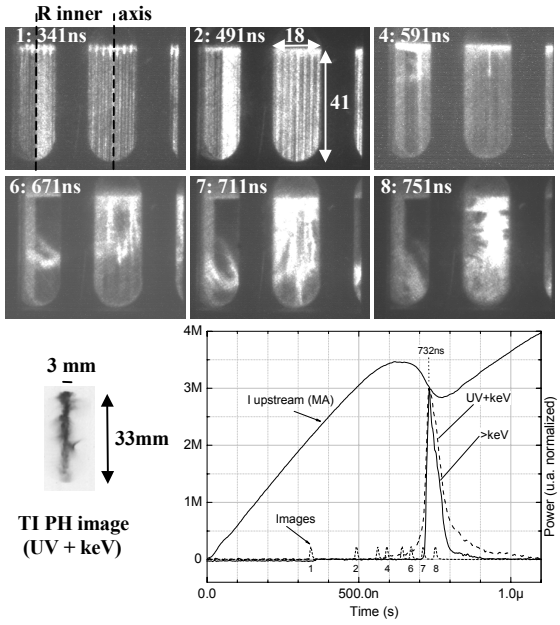

Fig. 1. Overall behavior of a nested arrays µs pinch (#485: D120/60 mm, 144/72 wires 10.4 µm diam.) with visible and TI X-UV images and radiation pulses

A qualitative spatial information on the final X-UV shape and dimension of the pinch is given by the pin-hole imager located at a different line of sight (90° from framing camera). Some qualitative observations can be done. On visible images, a homogeneous lightening of the outer array wires and later in the pulse of the inner array are observed (around 300 ns according to other shots and streak camera data). This means that the shielding of the inner array by the outer array is not complete and that an inductive division exist significantly during the first third of the implosion time. A solid core on the outer wires is still visible 500 ns after the beginning of current (2nd image). A precursor plasma reaching the axis early during the implosion time can be seen on the 4th image (590 ns); this effect was even clearer on previous single array shots. So, as shown by others laboratories in the 100–300 ns regime, a long ablation phase of wires is observed, and implosion occurs with individual structures created by the plasma expansion from the discrete wires. A plasma radial 'tail' propagating from top to bottom is also visible during the implosion (left aperture in images 4,6&7). This phenomenon is more or less present according shots, and could be attributed to power flow issues associated with current losses.

Vacuum Power flow: This last question led us to define dedicated configurations to allow better measurements of the downstream current with B-dots protected from direct radiation and/or plasma. The mechanical design that extend the downstream coaxial line is presented in Fig. 2.

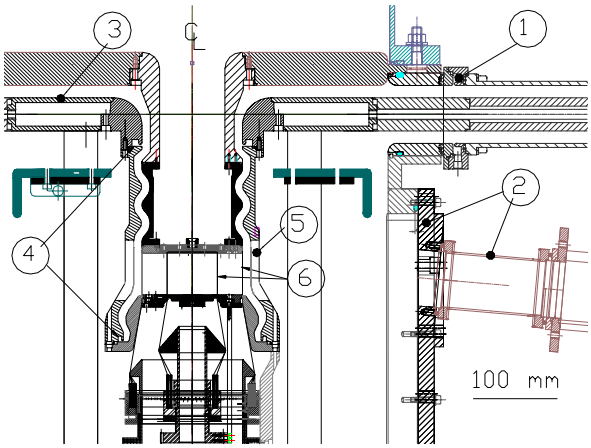

Fig. 2. Mechanical design for currents measurements (DS 120/60mm): 1 – Rogowsky (line current), 2 – line of sight, 3 – convolute, 4 – B-dots, 5– return current can (HV anode), 6 – wire arrays (top at ground)

Figure 3 presents the total current upstream the convolute (Rogowsky's sum) and upstream and downstream of the pinch measured with 3+3 B-dots. The 2 later currents are divided by 1.035 to fit the maximum of the current before the convolute. This correction can be consistent with the uncertainty in the B-dots calibration process. These measurements show there isn't significant losses during the implosion time, less than a few percents according to the measurements precision, in this region from upstream of the convolute to downstream of the load. Vacuum flashovers appear, but after the implosion: flashover in the convolute 200 ns after the pinch time, flashover in the coaxial line above or along the pinch close to the

maximum compression time (see separation of those 3 currents on Fig. 3).

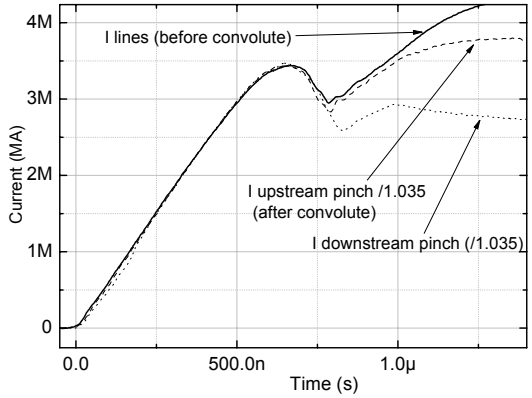

Fig. 3. Currents on a nested wire-arrays load (#505 DS 120/60 mm, 144/72*10.4 µm Al wires, extended. can)

So it's difficult to relate the plasma tails in visible images to power flow issues and it is not clear why the pinch is less bright and more diffuse at the bottom than at the top. More experiments will be done to complete this analysis and find conditions for a better axial homogeneity of the pinch: changing the polarity of wire arrays (negative up to May 2004, positive after May 2004), reducing the load length from 5 to 3 cm, etc…

Results overview: Very different regimes were explored from very light outer arrays (#488, #492 and #491) to more classical balances where $m_{outer}/m_{inner} \sim 2$ and diameters ratios $d_{outer}/d_{inner} \sim 2$. Wire arrays designs, maximum current before pinch, implosion time, radiated energies and powers: total and above 1 keV, are given in TABLE I for the best single array shot and for the double arrays shots. Four of the DS results are not included here because on 3 of these, we used non recessed B-dots in-between arrays to evaluate the current repartition that in fact, proved to disturb significantly the dynamic behavior and the X-rays outputs (i.e. keV yield output divided by 2). On the 4th one that was dedicated to evaluate reproducibility (as #485 and #496), some wires (2 to 3) were broken before shot on both arrays and decreased the keV expected yield by 30%.

Total powers given in Table 1 are deduced from bolometry measurement and hypothesis of a triangular pulse.

Xrays yields (from bolometer and PCD's integrals) given in this table are subjected to several comments:

– Due to the angle of the lines of sight, the observed fraction of the pinch is the upper part and represents typically less than 70% of the total height. On shot 506 with extended return current can, this number is increased to 90% and the Kshell yield is reduced from more than 25%, pointing out that the number given with the more reduced field of view could be optimistic because of the weaker part of pinch at the bottom that is not seen by the detector.

– It can be noted than a 40% reduction on the height of pinch (only one shot #502 done with 30 mm height) gives only a 15% reduction on the >1 keV yield, with a better axial homogeneity as shown by time integrated X-ray images.

According to this limited number of shots, maximum current before compression is mainly related to the outer array and the increase of its mass allows to improve the kinetic energy that can be coupled to the load with a consequent increase of the keV radiation output up to around 14 kJ (for the heaviest outer shell on a 164 µg/cm inner shell).

The optimum compression time seems to be around 800 ns with the best outputs for a balance of mass around 2 or more for the two main tested diameters configurations: 140/74 mm or 120/60 mm.

Table 1. Load parameters and measured output for single shell (SC) and double shell (DS) configuration of Al wire arrays

Shot	Configuration: shell diam. in mm, wires numbers and diam. (array mass in mg)	I_{max} (MA)	Implos time (ns)	Mean total P (GW)	E tot. (kJ)	Power >1 keV (GW)	E > 1 keV (kJ)
476	SC120–152*10.4 (1.74)	3.65	786	1123	73?	104	4.6
485	DS120/60–144/72*10.4 (1.64/0.82)	3.46	730	1922	98	271	11
486	DS140/74–108/72*10.4 (1.24/0.82)	3.40	755	1175	74	271	12
488	DS140/74–16/72*10.4 (0.18/0.82)	2.80	643	2960	74		5.2
491	DS120/60–64/72*10.4 (0.73/0.82)	3.07	678	1719	98	299	7.6
492	DS140/74–36/72*10.4 (0.41/0.82)	3.00	665	1125	72	183	7.1
493	DS140/74–108/48*10.4 (1.23/0.55)	3.40	730	1121	65	241	10.6
495	DS140/74–144/72*10.4 (1.65/0.83)	3.67	800	1833	88	352	14.1
496	DS120/60–144/72*10.4 (1.64/0.82)	3.40	718	1273	84	188	11.5
502	DS120/60–144/72*10.4 (0.99/0.5) h30mm	3.60	743	3830	72	263	9.3
504	DS140/74–192/48*10.4 (2.2/0.55)	3.71	805	1546	70.5	391	13.3
505	DS140/80–120/40*10.4 (1.38/0.46)	3.59	772	1226	76	123	7.3
506*	DS120/60–144/72*10.4 (1.64/0.82)	3.44	747	1701	83	206	8

* Shot 506 with external return current can extended to perform downstream pinch current measurements.

4. 0D Simulations

Beside more sophisticated 2DMHD simulations, 0D slug model coupled with MQK and TWG radiation models is used at CEG in order to analyze shot data and improve load design. This slug model is an evolution of the model proposed by A. Velikovich [10] with momentum exchange between the two arrays during the collision adjusted thanks to a collision factor *f*.

To model the long ablation phase for the outer array and the presence of a precursor plasma in the interior of the array leading to a snowplow-like implosion, the slug model is also divided into two phases. In the first one, the movement of the outer array is forbidden an we use the ablation model described by Lebedev in [11] to determine the time when the implosion starts. The equation of this phase is so:

$$V.\frac{dm}{dt} = -\frac{\mu_0 . I^2}{4\pi R_0} \text{ until } \delta m(t) = C_s \cdot m_{\text{ini}}.$$

The coefficient V and C_s have been obtained by fitting the experimental data of shot 496. Their values are $V = 15$ cm/μs and $C_s = 35\%$. They will be checked in the future on a bigger set of shots and experimental datas.

The second phase describes the movement of the two arrays after the ablation. Its equations are those presented in [10] except for the outer array momentum derivative which becomes:

$$m(t)\frac{d^2r}{dt^2} - 2\pi r\rho(r)\left(\frac{dr}{dt}\right)^2 = \frac{\partial}{\partial R_1}\frac{1}{2}LI^2;$$

$$\frac{dm(t)}{dt} = -2\pi r\rho(r)\frac{dr}{dt}.$$

As explained in [11], the initial mass in the piston does not correspond to the total mass left in the cores after the ablation phase; we achieve a good fitting with experiment (shells radii determined by the streak camera for the parts visible througth the return current can, see Fig. 4) by taking only 20% of the remaining mass in the inital piston.

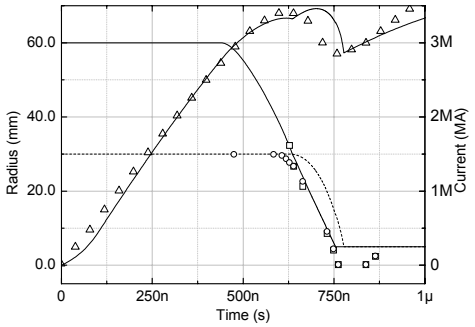

Fig. 4. Calculated (lines) and experimental #496 (dots) values for total current and trajectories of the arrays

By keeping all the parameters described before constant, we manage to fit the experiments done in term of K-shell outputs, implosion time and maximum current by adjusting the collision factor *f*. To explain that, we made the assumption that because of different inductive division, the inner array wires don't explode at the same time in different shots and that the earlier they explode, the less transparent is the inner array when the collision occurs. By estimating roughly the explosion time of the inner array by

$$\int_0^t R.I_{inner}^2 dt = \left(L_v + L_f\right)\cdot m_{inner} \ ,$$

we found that the dependance of the collision factor with this value is a linear law (Fig. 5).

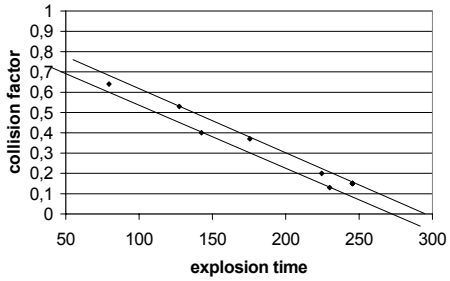

Fig. 5. Collision factor needed to fit nested wire arrays experiments versus calculated explosion time of the inner array

In summary, production of high X-ray yield with microsecond implosion time scale of aluminum nested wire arrays was demonstrated. Up to 14 kJ of energy above 1 keV was obtained, with pulse widths of 30–50 ns and total yield around 100 kJ. The optimization of this keV yield output is still underway. The progress in the understanding of these complex loads and, in addition, the increase, in the very near future of the stored energy of the generator should lead us to obtain a powerful μs PRS at a much reduce cost.

References

[1] C.A. Coverdale et al., Physical Review Letters **88-6**, 65001-1–65001-42002 (2002).

[2] P.L. Coleman et al., *Laser and Particle Beams,* 2001, pp. 409–441.

[3] A. Shislov et al., *14th IEEE International Pulsed Power Conference*, 2003, pp 1447–1450.

[4] F. Hamann et al., *in: Proc. of International Conference of Plasma Science,* Baltimore, June 2004, to be published.

[5] C. Mangeant et al., *this conference*.

[6] R.B. Spielman, C. Deeney et al., Rev. Sci. Instr. **70-1**, 651–655 (1999).

[7] G.A. Chandler, D.L. Fehl, R.B. Spielman, *Sandia Internal Report*, Albuquerque, USA, 1996.

[8] *Team Specialty Products*, Albuquerque (NM), USA.

[9] F. Bayol et al., *in: Proc. of Beams Conference,* St Petersburg, Russia, July 2004, to be published.

[10] A.L. Velikovich et al., Physics of plasma **9-4**, 1366–1380 (2002).

[11] S.V. Lebedev et al., Physics of plasma **8-8**, 3734–3747 (2001).